# High Voltage Stacked Diode Package with Integrated Thermal Management

Lauren M, Boteler, Miguel Hinojosa,
Valerie A Niemann
U.S. Army Research Laboratory
Adelphi, MD, USA, 20783
lauren.m.boteler.civ@mail.mil

Steven M. Miner
U.S. Naval Academy
Annapolis, MD, USA

David Gonzalez-Nino
University of Puerto Rico
Mayaguez, PR, USA

## ABSTRACT

Recent fabrication of high voltage (15-30 kV) single-die silicon carbide (SiC) power devices have necessitated advanced packaging methods to realize their full potential. This work discusses the limits of current power electronics packaging and explores an option of stacking high voltage Junction Barrier Schottky (JBS) diodes with integrated cooling. The new package has been designed, fabricated, and tested showing it can handle continuous and pulsed loads up to 21 kV. Dielectric fluid tests and pulsed measurements were also performed. Co-design and co-engineering methodologies were implemented during the initial design process. A key component to the co-designed module is a multi-functional connector (MFC) which acts as a mechanical, thermal and electrical contact at the same time. Adding enhanced functionality to package parts can potentially allow significant improvement in size, weight, cost, reliability, and performance.

**KEY WORDS:** co-design, multi-functional components (MFCs), electronics packaging, stacked die, JBS, silicon carbide (SiC), dielectric fluid, power electronics

## INTRODUCTION

The Army is moving to a more electric force with multiple pulsed and continuous ultra-high voltage applications. State-of-the-art 4H-SiC power semiconductor devices are currently under development for an increasing number of Army applications including microgrids, communications, survivability, and lethality systems. Single die, ultra-high voltage (UHV) silicon carbide IGBTs, MOSFETs, and Junction Barrier Schottky (JBS) diodes have been developed under the Army-Wolfspeed (A Cree company) partnership with operating voltages in the range from 15-30 kV [1-5]. However, packaging these high voltage devices has proven to be challenging since standard packaging methods cannot withstand the high voltages in a compact form. Often, the current power module packaging technique comprises devices soldered to a DBC (direct bonded substrate) substrate which is soldered to a heat spreader that is attached by a thermal interface material (TIM) to a heat sink. This packaging method has three primary failure locations [6-8]: the DBC substrate [9-10], wirebonds, and large area attach. A DBC substrate is two layers of copper sandwiching a thick ceramic, either aluminum nitride (AlN) or aluminum oxide ($Al_2O_3$). The present standard ceramic thickness is 0.025" which can withstand less than 10 kV reliably. DBC having 0.040" thick ceramic is also available which can withstand <15 kV. Thicker DBC (specifically with a substrate based on silicon nitride) is being developed but is very costly. This leads to the need to develop a reliable high-voltage module which eliminates the DBC. Therefore, alterative packaging methods are necessary.

Standard power electronics packaging follows a linear design process: initially, a circuit design is developed by an electrical engineer, then a mechanical engineer designs a reliable package, and finally a thermal engineer determines the appropriate heat sink for the application. Instead, there is a need for packages to be co-designed such that the mechanical, electrical and thermal aspects are accounted for at the same time in the initial design process. This allows packages with improved size, weight, cost, and performance. The package shown in this work is an example of a co-designed package where its components provide multiple functions and thus overall improvement.

The authors previously designed, built and tested the high voltage stacked diode package [11] shown in Fig. 1 and Fig. 2. To increase package voltage, diodes were assembled in a series configuration. This work explores stacking diodes to increase voltage while improving the size, weight and power density of the module. The two 15 kV stacked diodes are shown in the center. The prototype package was 10X smaller and weighed significantly less than the equivalent discrete diode packages. The completed package with the stacked diodes showed avalanche breakdown occurring at 29 kV. During a clamped-inductive load test the stacked diodes showed lower parasitic capacitance, faster reverse recovery time, and lower turn on energy as compared to the discrete diode packages. This package showed excellent performance for pulsed or single use applications; however, many SiC applications involve high power and continuous operation which requires the ability to remove heat.

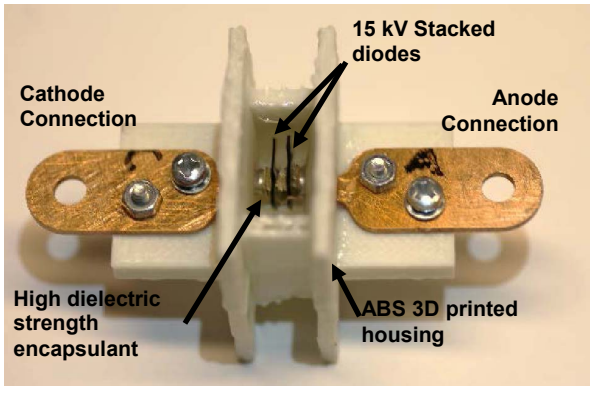


Fig. 1. Picture of the previously completed stacked diode assembly with the main features called out. [11]

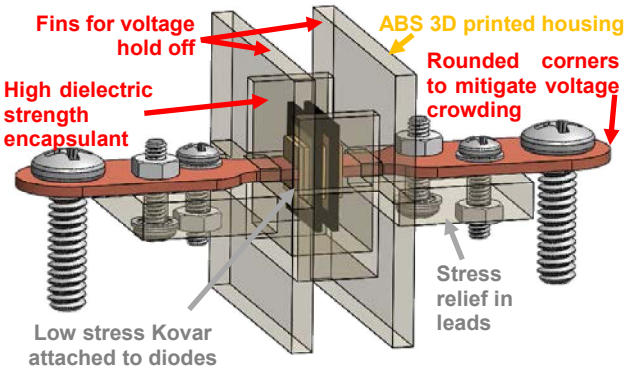


Fig. 2. Schematic of the previous stacked diode assembly. Red text indicates the high voltage aspects. Grey text represents the reliability advantages. Gold text shows the cost benefits. [11]

## HIGH VOLTAGE PACKAGE WITH INTEGRATED COOLING

While the previous module showed significant benefits in size, reliability, and electrical performance, it did not effectively remove heat. There exist many high voltage applications where this is not a concern, however the Army also needs a high voltage module which can be used in high power pulsed or continuous use applications. Therefore, leveraging the knowledge gained from the previous module design, fabrication and testing, the module was redesigned, and a heat sink was implemented into the package. The completed module is shown in Fig. 3. It consists of two 15 kV SiC diodes electrically connected in series, allowing up to 30 kV operation. There are two electrical contacts on each side of the box for the anode and cathode. Fluid ports at the top and bottom of the box to allow a dielectric fluid (Novec 7500) to flow directly over the diodes and actively cool the assembly.

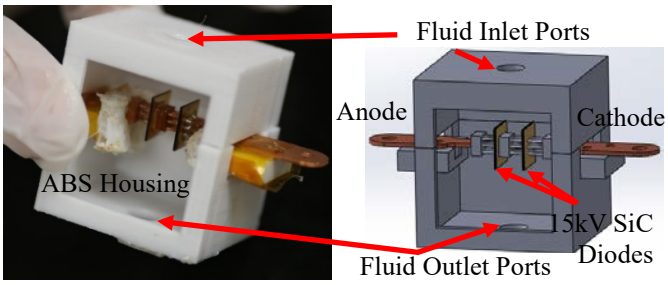


Fig. 3. Fabricated high voltage module with integrated cooling. Image shows location of fluid ports as well as the cathode and anode of the diodes, stacked in series.

The new package has eliminated the three primary failure locations of existing power electronics modules: the DBC, wirebonds, large area attaches. Cost is reduced by eliminating the expensive DBC and using a low-cost ABS (acrylonitrile butadiene styrene) additively manufactured housing. ABS was used as a proof of concept at low temperatures; in a commercial package, a more robust plastic can be used.

A primary innovation of the package is the copper structures that connects the devices together, shown in Fig. 4. Typical packages utilize wirebonds whose sole purpose is electrical contacts and heat sinks whose sole purpose is removing the heat. This multi-functionality connector (MFC) instead acts as the electrical, mechanical and thermal contact simultaneously. This multi-functionality of components is a key component of co-design. By designing connections with multiple purposes, a package can be realized with improved size, weight and performance.

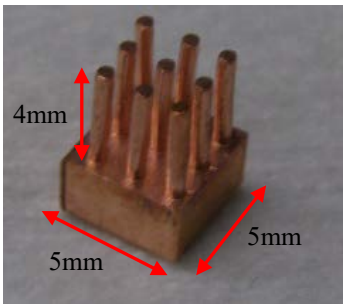


Fig. 4. The multi-functionality connector (MFC) is a key enabling component of the high voltage module.

### Package Fabrication

Fabrication of the final package is detailed below.

**Step 1:** Fabricate the three components required for assembly: (1) multi-purpose connectors (MFCs), (2) electrical leads and (3) alignment fixtures. The MFCs, shown above in Fig. 4 were cut out of a larger commercially available heat sink, the SLF-1 Ultra by Enzotech [12]. This heat sink was chosen because it is made of pure copper which has high thermal conductivity and electrical conductivity. In addition, the fin dimensions fit well with the diode size allowing a 3x3 array of 4 mm tall fins on each side of the die. Three identical MFCs were required for each module.

The electrical leads, shown in Fig. 5, were machined out of a copper sheet and designed to attach to the flat top of the MFCs. The rounded corners were required to reduce voltage concentrations and the single larger hole was designed for external electrical connections allowing screw terminal or solder attachment. The two smaller holes were designed for mechanical attachment to the housing.

Fig. 5. Fabricated copper electrical contact with rounded corner to mitigate voltage crowding and holes for electrical and mechanical contact.

The final machined components are the alignment fixture shown in Fig. 6. Alignment during fabrication is critical in a stacked assembly. Ensuring the MFCs are aligned properly to the top-side of the diode reduces the chances of voltage breakdown, ensures mechanical robustness, and improves heat transfer since misalignment could cause the connectors to contact the isolation perimeter on the device. Four vertical alignment parts were designed to ensure proper placement of

the die stack and the connectors. A square ring was placed around the perimeter to secure the parts during the die attach curing process.

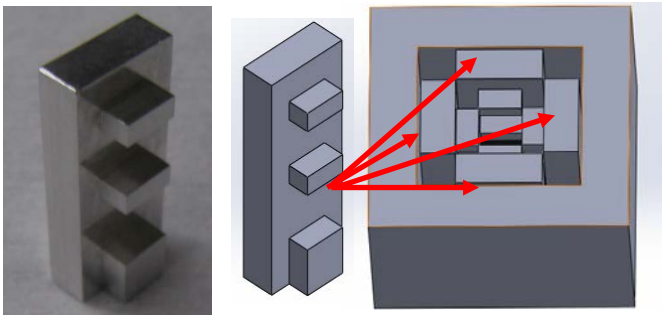

Fig. 6. Schematic depicting the vertical alignment parts as well as the square perimeter ring used to align the stacked structure during the die attach process.

**Step 2:** Bond the backside of each 15kV diode to an MFC. A high conductivity silver epoxy, EPO-TEK EK1000, was chosen to attach the diodes to the MFCs. To reduce the potential for alignment error, first the backside of each diode was attached to an MFC, as is shown in Fig. 7. The epoxy was painted onto each of the nine fins (Fig. 7a), then the MFC was placed into the alignment fixture, ensuring tight contact to three of the vertical walls (Fig. 7b). Once three walls were placed, the device was gently slid into the fixture and dropped onto the uncured silver epoxy, subsequently applying a slight amount of pressure to allow good contact (Fig. 7c). The fourth vertical wall is then slid into place and a square perimeter ring was put into place around the structure to prevent movement during the curing process, as is shown in Fig. 7d. The entire stack was then transferred into an oven to cure the epoxy.

**Fig. 7a**: Apply silver epoxy

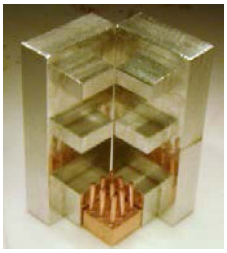

**Fig. 7b**: Place MFC in fixture.

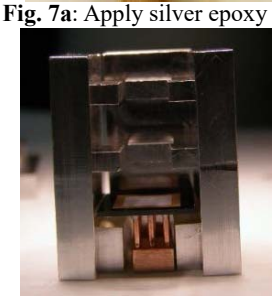

**Fig 7c:** Align diode

**Fig 7d:** Assemble fixture

Fig. 7. The four sub-step assembly process to attach a single die to an MFC ensuring proper alignment of the second step of the module assembly process.

This process was then repeated for the second diode except that the MFC was flipped and the solid part is attached to the backside of the diode. The completed pair is shown in Fig. 8.

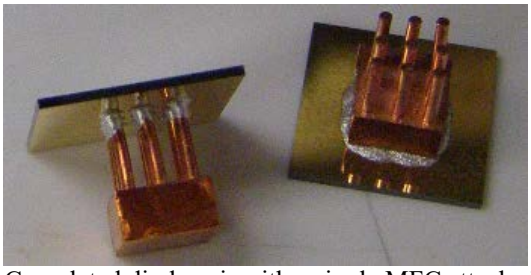

Fig. 8. Completed diode pair with a single MFC attached

**Step 3:** Align the complete stack and bond. Using the same alignment fixture as was used in Step 2, assemble both connected diode/MFC pieces as well as a third MFC ensuring proper placement and alignment, shown in Fig. 9. The third MFC is located on the top of the upper diode.

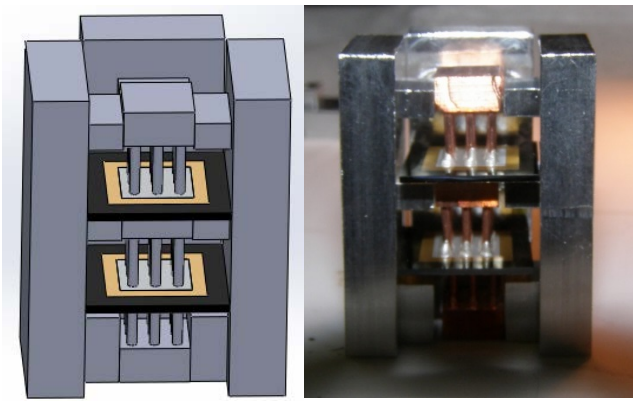

Fig. 9. Image depicting how the diodes and MFCs are stacked inside the alignment fixture during the final bond.

After bonding in the oven and removing the fixture, the complete assembly is shown in Fig. 10. The stack should have the solid side of the MFC at both ends and pin fins should be attached to the top of each diode.

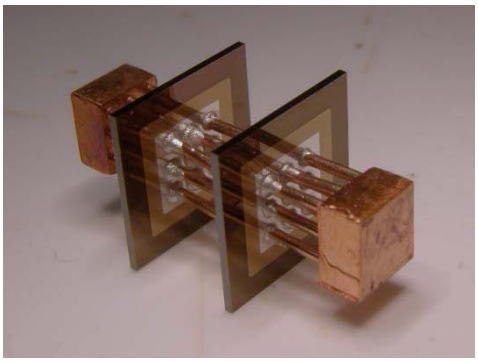

Fig. 10. Completed stacked structure after die attach with two diodes and three MFCs.

**Step 4:** Attach the leads. Using a wood fixture, to help with alignment, shown in Fig. 11, the leads are attached to each end of the stack using SnPb solder.

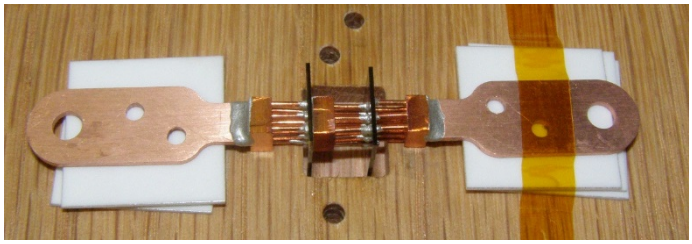

Fig. 11. Solder fixture used to align the copper leads to the completed stacked structure and attach.

The full central structure is shown in Fig. 12.

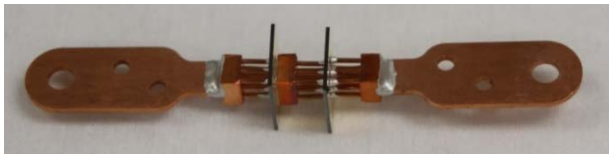

Fig. 12. Completed central structure.

**Step 5:** Coat interior structure with dielectric coating. To increase the voltage breakdown, the entire interior structure (diodes, die attach, and MFCs) was coated with a high dielectric strength material (Loctite M-31CL). The epoxy was first heated to reduce its viscosity and then applied to the structure using a pipette. The epoxy thickness is thin and variable across the structure and will act as a small thermal resistance.

**Step 6:** Attach housing. A smaller housing was first designed but had to be removed after initial hi-pot testing showed breakdown at <14kV. The second housing was designed to fit around the remnants of the first housing and allowed fluidic sealing, tube attachment, visual inspection, and sufficient distance to the device to negate the potential of voltage creep to the housing. The housing was made leak-proof by sealing the interior with a thin epoxy coating. Fig. 13a shows the placement of the central structure in the housing. Fig. 13b shows the tube attachment as well as the placement of the optical viewing window allowing visual inspection before, during and after testing.

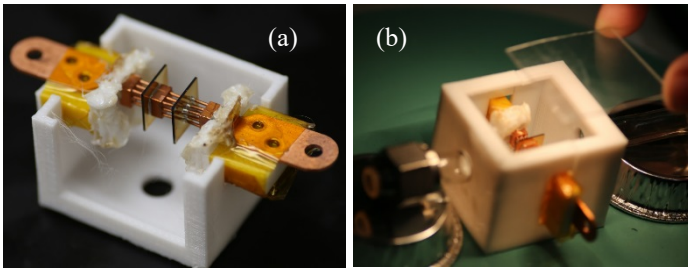


Fig. 13. Images of the housing assembly (a) depicts the central structure placement in the additively manufactured housing (b) Placement of the clear window after box was assembled and fluid ports attached.

## EXPERIMENTAL RESULTS AND DISCUSSION

### Dielectric Fluid Static Tests

Initially, a series of tests were performed on various dielectric fluids during both static and active fluid flow conditions. A simple dielectric test bed was fabricated in-house and is shown as an inset in Fig. 14. It consists of an additively manufactured box with two nickel-plated copper electrodes inserted into the box on opposing sides. The box was fluidically-sealed using an epoxy. The gap between electrodes was adjusted by reducing the length of the thin wires and the spacing was carefully monitored using calipers. A high potential (hipot) test was performed using a Spellman MP30 high voltage power supply which has a 30 kV maximum voltage rating, a 300 μA maximum current limit, and a programmable feedback control interface that connects to a LABVIEW computer. During the hipot dielectric tests the following fluids were evaluated in the laboratory: 3M Novec 7500 Engineered fluid, Clearco Silicone transformer oil (100% dimethyl polysiloxane), and Castrol 399 oil. Fig. 14 shows a plot of the voltage breakdown as a function of electrode spacing for the various fluids.

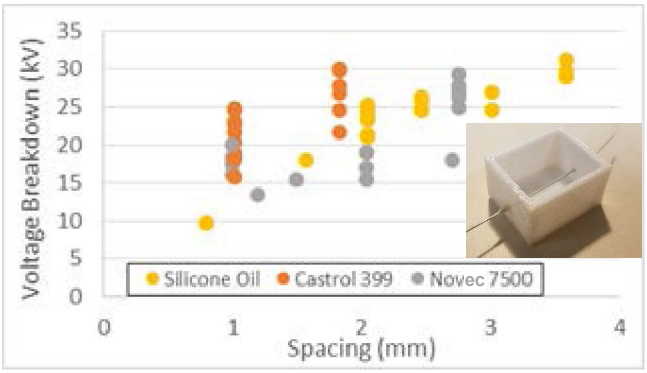


Fig. 14. Plot of the voltage breakdown as a function of electrode gap spacing for static fluid tests.

Preliminary results show that there was significant variability in the voltage breakdown as the gap size increased. Even at the same spacing with the same fluid, repeated tests showed variability. The cause of these variations could be attributed to the purity and age of the tested fluids, the formation of carbonized filaments resulting from test to test (an effort was made to clean the contacts), and from microscopic surface roughness variations in the electrodes that lead to localized electric field crowding. Nevertheless, while these tests were not exhaustive of all the potential variability, they did lead to a design with a significant safety factor to account for the variability. The fluid chosen for the module remained 3M Novec 7500 based on its acceptable dielectric performance, heat transfer properties, thermal stability, viscosity, environmental impact, and electronic compatibility.

### Dielectric Active Fluid Testing

In addition to static testing, a series of hipot tests were performed to determine if active fluid flow would change the dielectric properties of the fluid. Fig. 15 shows the structure designed for the experiment. It was similar to the static fluid

fixture but had a clear window on the top that is securely mounted using a gasket onto the base as well as fluid inlet and outlet tubes that were connected to a flow loop containing Novec 7500.

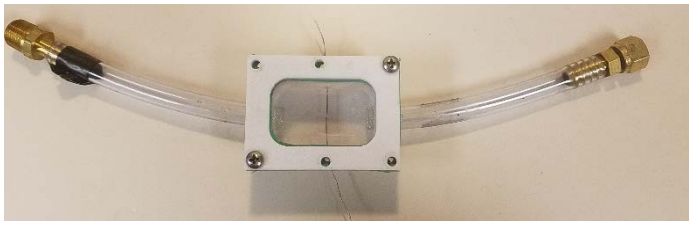

Fig. 15. Fixture used for high-potential active fluid test.

The results from the active fluid flow experiment are shown in Fig. 16. The exact flow rate was not measured but a qualitative no flow through fast flow was determined based on a completely closed through completely open valve. In general, the variability seen was not dependent on flow rate and the flow rate did not have a large impact on the dielectric strength of the fluid.

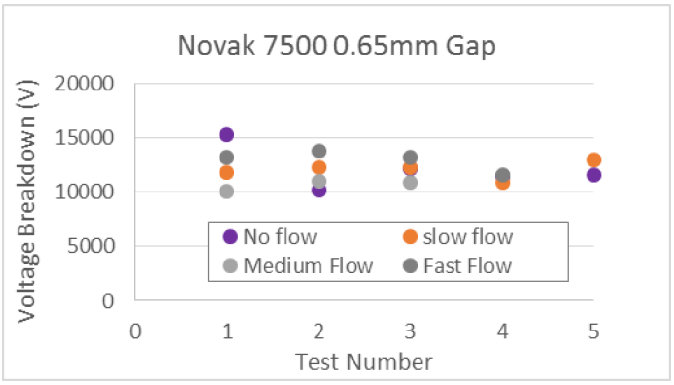


Fig. 16. Plot of the voltage breakdown for various flow rates at 0.65 mm gap. The x-axis is repeat tests of the same flow rate.

**Blocking Tests and Forward Conduction of Diode Modules**

Fig. 17 shows the three different types of modules each containing two equivalent 15 kV diodes assembled in a series configuration to create a 30 kV module. The discrete diode package consists of two independently packaged 15 kV diodes which are then connected externally. The uncooled stacked diode package was previously compared to the discrete diodes showing a 10X reduction in size as well as improved switching performance [11]; however, the ability to remove heat was limited. Therefore, the module shown in this paper (cooled stacked) was designed and fabricated to take advantage of the stacked approach with an integrated heat sink.

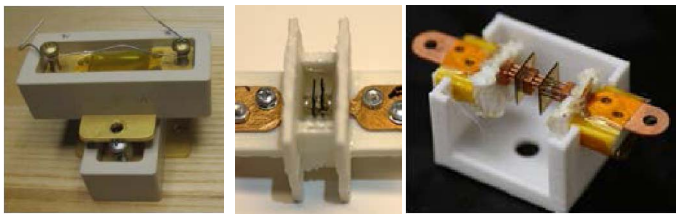

Discrete Diodes | Uncooled Stacked | Cooled Stacked

Fig. 17. Three modules used for comparison testing each consisting of the same two 15 kV diodes.

The first series of tests performed on the modules included the pulsed dielectric breakdown and the continuous-blocking leakage current tests. In the pulsed dielectric breakdown test, the voltage was stepped up carefully until the semiconductor goes into avalanche breakdown, the package material breaks down, or its current reaches a predetermined compliance limit. In the continuous-blocking current test, the devices were kept in blocking mode for an extended time at 60-70% of their maximum holdoff voltage. The tests were performed in the same test bed as the hipot fluid tests. The dielectric fluid of the cooled stacked module remained stagnant due to the short duration, minimal heating of the devices, and also since it was shown that it does not significantly affect the dielectric properties. The second column of Table 1 shows the results of the continuous-blocking test indicating the voltage at which each of the three modules could block for 5 minutes. The third column of Table 1 shows the voltage at which the threshold current of 20 µA was reached during a hipot test. The last column in the table shows the suspected failure mode. The devices are capable of withstanding 15 kV each; therefore, a breakdown <30 kV was assumed to be due to the packaging and not the devices. The uncooled stacked diode module reached almost 30 kV before avalanche breakdown indicating the devices were breaking down before the packaging. In each test the uncooled stacked module could handle the highest voltages. The cooled stacked modules performed similarly to the discrete diodes.

Table 1: Summary of results for dielectric breakdown tests

| Device: | Continuous (kV) | Failure @ 20 µA (kV) | Failure mode: |
|---|---|---|---|
| Discrete Diodes | 20 | 21.25 | Package |
| Uncooled Stacked | 25 | 29.25 | Avalanche |
| Cooled Stacked | 20 | 20.36 | Package /Fluid |

The next set of tests performed on the three modules included forward-conduction tests. The forward-conduction I-V characteristics were measured using a Tektronix 371B high-power curve tracer. The I-V results are shown in Fig. 18. Diode voltage drop increases with temperature for a given current. The plot shows that the uncooled stacked package (orange) has a higher voltage drop at any given current as

compared to the other two packages (discrete and cooled stacked) indicating it is heating up more. Due to the relative inability to remove heat from the uncooled stacked package, its diodes became more resistive as the heat was trapped between the two diodes showing a higher voltage drop. The discrete diode package and the cooled stacked package showed similar results with slightly better performance by the cooled stacked module.

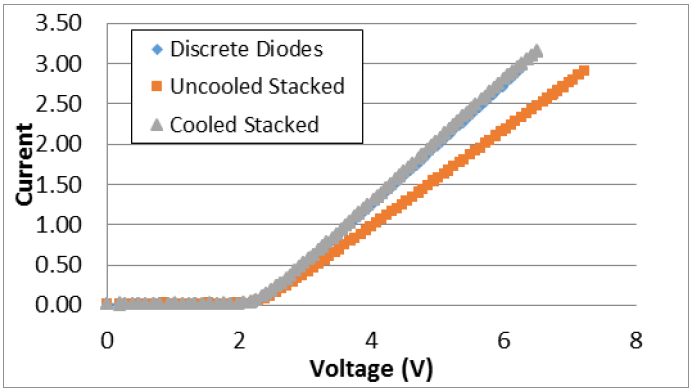


Fig. 18. Forward-conduction IV plot for the various diodes.

**Clamped-Inductive Tests**

The next set of tests determined the dynamic characteristics of the actively-cooled stacked diodes using a clamped-inductive circuit as shown in Fig. 19. This circuit utilized a 40 kV, 4 kJ/s TDK-Lambda variable power supply (V1) to charge an 8 µF capacitor bank (C1) through a 25 Ω resistor (R1). A 20 kV, R&D-grade, SiC IGBT (U1) was utilized to switch the 10 mH inductor (L1), and a 1 kΩ ceramic resistor (R2) was used to maintain the peaking current low. The devices under test (D1-D2) protect the IGBT from the inductor's stored energy and they were connected in parallel with respect to L1 and R2.

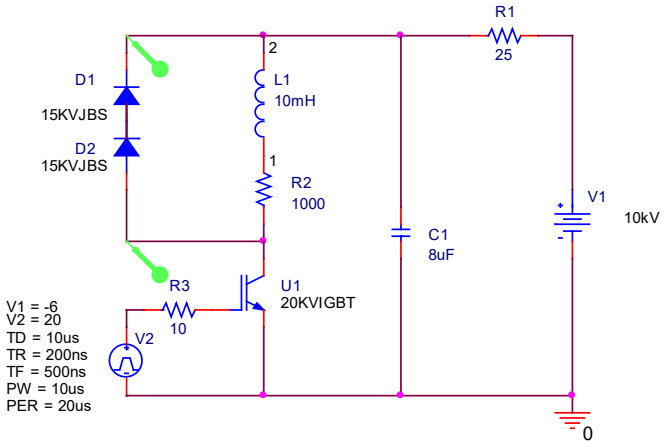


Fig. 19. Clamped-inductive circuit to test diodes.

The evaluation circuit was operated from 6 kV to 10 kV with pulse widths ranging from 20 µs to 100 µs. The duty cycle for each pulse was varied from 10 percent to 80 percent. Fig. 20 and Fig. 21 show a snippet of the voltage and current waveforms, respectively, for a 20 µs, 50 % duty cycle, pulse. These plots show good characteristics of the module.

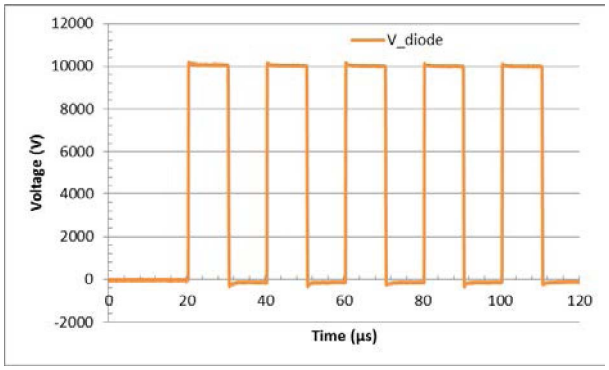


Fig. 20. Diode voltage as a function of time.

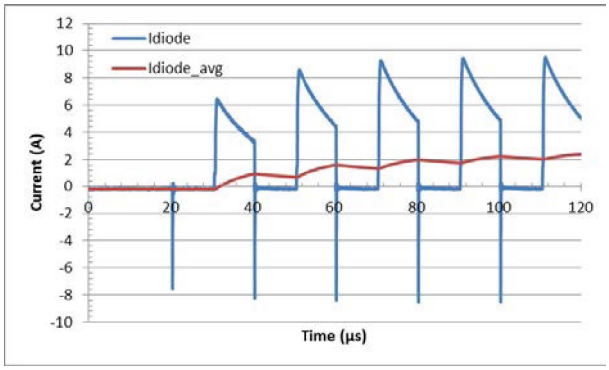


Fig. 21. Diode current as a function of time.

Table 2 shows a summary of the tests performed on the Novec-cooled diode stack using the clamped-inductive circuit for a mass flow rate of 0.025 kg/sec. The tests were limited to a conservative value of 10 kV because of the limited number of IGBT switches available. These results indicate the ability to continuously switch these diodes at high voltages. Future tests will include operating voltages up to 20 kV and beyond.

Table 2: Summary of clamped-inductive tests.

| Bus Voltage (kV) | Pulse Width (µs) | No. of shots | Duty Cycle % |
|---|---|---|---|
| 6 | 20 | 1-5 | 50 |
| 7 | 20 | 1-5 | 50 |
| 8 | 20 | 1-5 | 50 |
| 9 | 20 | 1-5 | 50 |
| 10 | 20 | 1-500 | 10-80 |
| 10 | 100 | 1-500 | 10-80 |

**NUMERICAL RESULTS AND DISCUSSION**

Due to the complexities of measuring device temperatures during high voltage pulsing, a series of thermal models were run to estimate the temperature using SOLIDWORKS Flow Simulation, a computational fluid dynamics tool. This particular solver used the Finite Volume Method to solve the Reynold's Averaged Navier-Stokes equations. This is a good conjugate heat transfer problem where the fluid and solid solutions are generated simultaneously. The mesh for the results presented here contain 291,773 fluid elements and

153,898 solid elements. Mesh convergence was evaluated by increasing the number of cells by 50% in both the fluid and solid portions of the model resulting in no significant difference, so the coarser mesh was used. The complexities include the inability to incorporate temperature sensors (thermocouples, RTDs, etc.) into the package as well as the challenges associated with measuring electrically. Also, due to the lack of visual access to the top surface of the devices, using a thermal camera was not an option. The modeling structure used is shown in Fig. 22. A heat flux of 15 W/cm$^2$ was applied at the center active area of the diode (5 mm x 5 mm area).

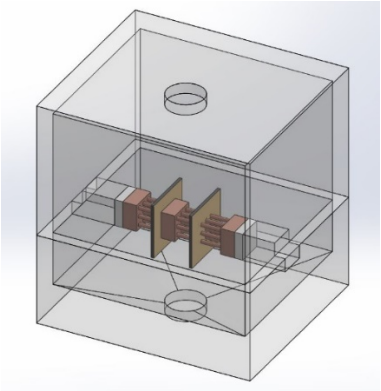

Fig. 22. Structure used for thermal and fluid modeling analysis in SOLIDWORKS.

One of the higher powered clamped inductive load tests occurred at 10 kV, 20 µsec pulse, and 50% duty cycle which equates to a 15 W/cm$^2$ average power dissipation for a mass flow rate of 0.025 kg/sec,. The model shows that under these conditions, the device temperature rose around 14°C with a pressure drop of 210 Pa. The thermal profile, shown in Fig. 23, illustrates the fact that having the base of the fins against the diode helps spread and remove heat from the diode. As a result, the right diode is hotter than the left.

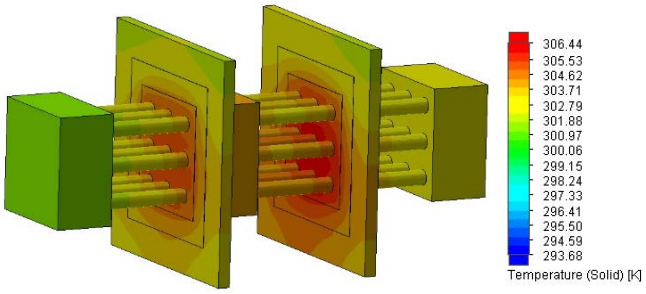


Fig. 23. Thermal modeling results estimating the device temperature during the clamped inductive load tests at 15 W/cm$^2$ power dissipation and 0.025 kg/sec flow rate

Velocity profiles are shown in Fig. 24 for 0.025 kg/sec. The front and side velocity images illustrate that the majority of the flow is directed through the middle of the stack, through the center MFC. Future designs could implement a more even flow distribution.

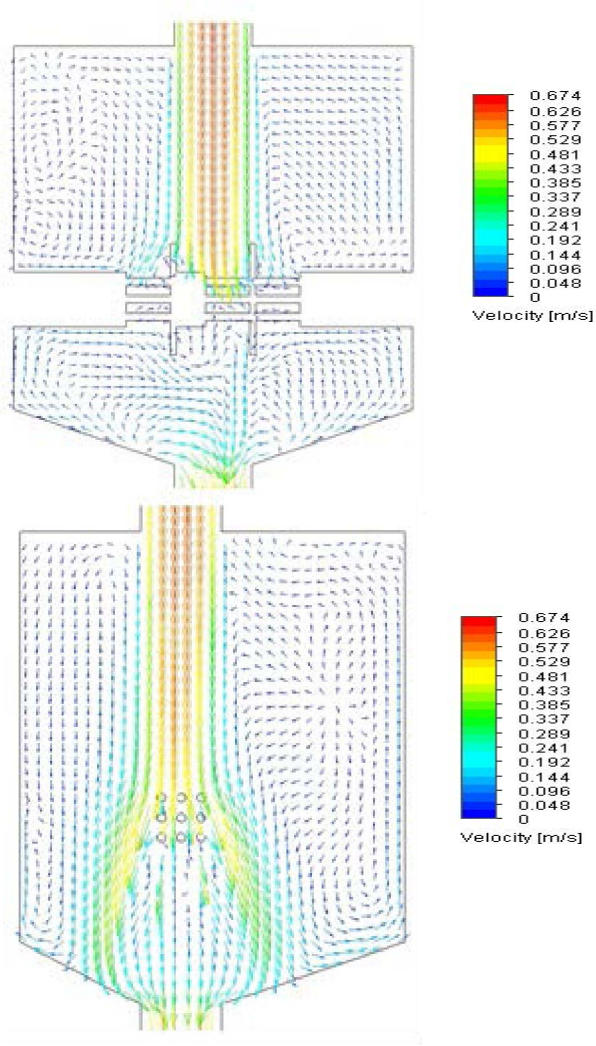


Fig. 24. Velocity vector results for center line cuts through the center of module and also through the center finned MFC.

A summary of the temperature and pressure drop results for various flow rates are shown below in Table 3 for power dissipations of 15 W/cm$^2$.

Table 3: Summary of numerical SOLIDWORKS results showing the rise in device temperature and pressure drop for a series of flow rates.

| Flow (kg/sec) | ΔT (°C) | ΔP (Pa) |
|---|---|---|
| 0.01 | 21.8 | 34.5 |
| 0.02 | 16 | 111.7 |
| 0.025 | 14.1 | 209.7 |
| 0.03 | 13.2 | 300.3 |
| 0.045 | 11.4 | 637.8 |
| 0.06 | 10.2 | 1099 |

## CONCLUSIONS

This work presented the first high voltage stacked diode package with integrated cooling capable of operation at

>20 kV. The fabrication assembly, electrical testing and thermal modeling were presented as part of this work. There is a need for advanced high voltage packaging due to the recent fabrication of high voltage SiC devices (>15 kV). A five-layer stack comprised of altering layers of copper fins and diodes was assembled. Electrical leads for the anode and cathode were soldered onto the external copper fin pieces and the entire assembly was epoxied into a 3D printed ABS box. Fluidic ports were also designed into the housing and a dielectric fluid was chosen to directly cool both the top and backside of each die. This module depicts the type of innovations that can be achieved when modules are designed using a co-design approach. The multi-functional connectors (MFCs) are parts of the package that act as the high voltage interconnects, heat sinks and mechanical attach simultaneously. This multi-functionality improves size, weight, reliability, cost and performance of power modules.

## ACKNOWLEDGEMENTS

The authors would like to thank colleagues at the U.S. Army Research Laboratory who, in various aspects, have helped support this effort including Bruce Geil, Claude Pullen, Morris Berman, Dimeji Ibitayo, and Ron Duane.

## REFERENCES

[1] McManus, K. “Silicon Carbide High-Voltage Power Technology”. Department of the Army Solicitation W911NF-13-R-0002. 2013.

[2] Wang, J.; Du, Y.; Bhattacharya, S.; Huang, A.Q., "Characterization, modeling of 10-kV SiC JBS diodes and their application prospect in X-ray generators," Energy Conversion Congress and Exposition, 2009. ECCE 2009. IEEE , vol., no., pp.1488,1493, 20-24 Sept.

[3] Hull, B.A.; Sumakeris, J.J.; O'Loughlin, M.J.; Qingchun Zhang; Richmond, J.; Powell, A.R.; Imhoff, E.A.; Hobart, K.D.; Rivera-Lopez, A.; Hefner, A.R., "Performance and Stability of Large-Area 4H-SiC 10-kV Junction Barrier Schottky Rectifiers," Electron Devices, IEEE Transactions on , vol.55, no.8, pp.1864,1870, Aug. 2008

[4] Tipton, C.W.; Ibitayo, D.; Urciuoli, D.; Ovrebo, G.K. "Development of a 15 kV bridge rectifier module using 4H-SiC junction-barrier schottky diodes", Dielectrics and Electrical Insulation, IEEE Transactions on, On page(s): 1137 - 1142 Volume: 18, Issue: 4, August 2011

[5] Brunt, E.V.;Cheng, L.; O’Loughlin M. J.; Richmond, J.; Pala, V.; Palmour, J.; Tipton, C.; and Scozzie, C.“ 27 kV, 20 A 4H-SiC n-IGBTs”. Silicon Carbide and Related Materials. Materials Science Forum. 2014

[6] Shammas NYA. Present problems of power module packaging technology. Microelectron Reliab 2003;43:519–27.

[7] Yannou, Jean-Marc, “Analysis of innovation trends in packaging for power modules,” proceedings of the 7th European Advanced Technology Workshop on Micropackaging and Thermal Management, February 1, 2012.

[8] H. Lu, Ch. Bailey, Ch. Yin. Design for reliability of power electronic modules. Microelectronics Reliability, 49 (2009), pp. 1250–1255

[9] Jürgen Schulz-Harder, “Advantages and new development of direct bonded copper substrates,” Microelectronics Reliability, Volume 43, Issue 3, March 2003, Pages 359-365

[10] L. Dupont, Z. Khatir, S. Lefebvre, S. Bontemps, Effects of metallization thickness of ceramic substrates on the reliability of power assemblies under high temperature cycling, Microelectronics Reliability, Volume 46, Issues 9–11, September–November 2006, Pages 1766-1771

[11] Boteler, L., Rodriguez, A., Hinojosa, M., & Urciuoli, D. (2015, October). High-Voltage Stacked Diode Package. In *International Symposium on Microelectronics* (Vol. 2015, No. 1, pp. 000225-000230). International Microelectronics Assembly and Packaging Society.

[12] http://www.enzotechnology.com/slf_1_ultra.htm, Accessed March 1, 2017.